Original Research Article

Feasibility of biology-guided radiotherapy using PSMA-PET to boost to dominant intraprostatic tumour

Mathieu Gaudreault [a,b,*], David Chang [b,c], Nicholas Hardcastle [a,b,d], Price Jackson [a,b], Tomas Kron [a,b,d], Michael S. Hofman [b,e], Shankar Siva [b,c]

[a] Department of Physical Sciences, Peter MacCallum Cancer Centre, Melbourne, Victoria 3000, Australia
[b] Sir Peter MacCallum Department of Oncology, The University of Melbourne, Victoria 3000, Australia
[c] Department of Radiation Oncology, Peter MacCallum Cancer Centre, Melbourne, Victoria 3000, Australia
[d] Centre for Medical Radiation Physics, University of Wollongong, NSW 2522, Australia
[e] Molecular Imaging and Therapeutic Nuclear Medicine; Prostate Cancer Theranostics and Imaging Centre of Excellence (ProsTIC), Peter MacCallum Cancer Centre, Melbourne, Victoria 3000, Australia

ARTICLE INFO

ABSTRACT

Background: Biology-guided radiotherapy (BgRT) delivers dose to tumours triggered from positron emission tomography (PET) detection. Prostate specific membrane antigen (PSMA) PET uptake is abundant in the dominant intraprostatic lesion (DIL). This study investigates the feasibility of BgRT to PSMA-avid subvolume in the prostate region.

Methods: Patients enrolled in the prospective randomized trial ProPSMA at our institution were included (ID: ANZCTR12617000005358). Gross tumour volumes (GTVs) were delineated on the PET component of a PET/CT scan from a standardized uptake value (SUV) threshold technique. Suitability for BgRT requires a strong signal-to-background ratio with a surrounding tissue free of significant PSMA uptake. The signal-to-background ratio was quantified from the calculation of the normalized SUV (nSUV), defined as the ratio between SUVmax within the GTV and SUVmean inside a 3D margin expansion of the GTV. The PSMA distribution surrounding the tumour was quantified as a function of the distance from the GTV.

Results: In this cohort of 84 patients, 83 primary tumours were included. Prostate volume ranged from 19 cm^3 to 148 cm^3 (median = 52 cm^3; IQR = 39 cm^3 – 63 cm^3). SUVmax inside the prostate was between 2 and 125 (median = 19; IQR = 11 – 30). More than 50% of GTVs generated with threshold between 25%SUVmax (median volume = 10.0 cm^3; IQR = 4.5 cm^3 – 20.0 cm^3) and 50%SUVmax (median volume = 1.9 cm^3; IQR = 1.1 cm^3 – 3.8 cm^3) were suitable for BgRT by using nSUV ≥ 3 and a margin expansion of 5 mm.

Conclusions: It is feasible to identify GTVs suitable for BgRT in the prostate. These GTVs are characterized by a strong signal-to-background ratio and a surrounding tissue free of PSMA uptake.

Introduction

External beam radiation therapy is one of the standard treatments for localised prostate cancer. Although effective, some patients experience a biochemical recurrence and among these patients, an estimated 20% or more will present with a local recurrence [1,2]. The most common choice of treatment for patients with local recurrence is a period of observation or androgen-deprivation therapy (ADT). However, ADT remains a palliative treatment that significantly affects the quality of life of patients. Local salvage procedures such as radical prostatectomy, high-intensity focused ultrasound ablation, cryosurgery or prostate re-irradiation are therapeutic alternatives that can be offered to highly selected patients but are associated with high risk of toxicity [3,4]. Approximatively 90% of local recurrences occur in the dominant intraprostatic lesion (DIL) which is the most prominent cancerous lesion within the prostate [5,6]. Recently, the FLAME randomized phase III

trial demonstrated that focal radiotherapy boost to the DIL in addition to standard prostate radiotherapy can improve biochemical disease-free survival in patients with localized prostate cancer [7].

Biology-guided radiotherapy (BgRT) (RefleXion Medical Inc., Hayward, USA) is a novel technology that uses positron emission tomography (PET) from patient's cancer cells to guide radiation treatment [8–10]. Potential advantages of this technique include real-time tracking of a tumour, which can improve the accurate targeting of the tumour, and the ability to treat many tumours in a single session [11–14].

Prostate specific membrane antigen (PSMA) PET tracers are now available for imaging of primary and metastatic prostate cancer [15–20]. This imaging technique has demonstrated superior sensitivity and specificity for prostate cancer diagnosis compared to conventional imaging [21–23]. Due to the particularly high PSMA uptake in the DIL, BgRT may be ideally suited to deliver a sequential boost to this region.

The ground truth for determination of DIL volumes is histopathology. Multiparametric magnetic resonance imaging (mpMRI) is the current imaging standard for evaluation of DIL volumes [24,25]. Variability in DIL volumes using this technique has been reported [26,27]. However, mpMRI acquisition is a long process and requires additional resources [28]. Recent studies have investigated determination of the DIL from PSMA uptake. DIL volumes were either first determined from mpMRI and then reproduced by %SUVmax threshold techniques [29–31], manually delineated on both MRI and PSMA PET datasets [32], determined first from histopathology specimens and then compared to manual and %SUVmax threshold delineation on PSMA PET images [33–35], or determined from a %SUVmax threshold technique without any other imaging references [36]. DIL determination from PSMA uptake may be advantageous; for instance, studies reported higher sensitivity and comparable specificity as compared with mpMRI determination [37–39].

This study investigates the feasibility of BgRT as a sequential boost to a PSMA-avid subvolume (PAS) in prostate cancer. We aim to quantify the proportion of tumours suitable for BgRT and describe the distribution of PSMA uptake in the surrounding normal tissue.

Materials and methods

All PSMA PET/CT scans of patients recruited in the ProPSMA prospective randomised trial (ID: ANZCTR12617000005358) acquired at our institution were considered for inclusion [23,40]. In this trial, patients received Gallium-68 (^{68}Ga) PSMA-11 PET/CT at the time of diagnosis for prostate cancer. PET/CT images were acquired with the Discovery PET/CT scanner 690 or 710, which is a PET tomograph with a 64-slice CT scanner (General Electric Medical System, Milwaukee, USA).

The prostate and bladder were segmented on the CT component of the PET/CT scan by a genitourinary radiation oncologist and a medical physicist in consensus by using the PSMA uptake on the PET component as a guide. Delineation was performed with the Eclipse treatment planning system (TPS) (v16.1, Varian Medical Systems, Palo Alto, USA). Misregistration between the CT and the PET component may be due to several factors, such as patient or physiologic movements. In all cases, distribution of the standardized uptake value (SUV) on the PET component was manually registered to contours on the CT component.

Quality control of ^{68}Ga SUV was performed in the ProPSMA study [41]. To allow patient intercomparison, SUV was subsequently normalized to body weight. Gross tumour volumes (GTV) for BgRT delivery were constructed on the PET component. To do so, GTVs were defined by segmenting PAS in the prostate region by using a %SUVmax threshold technique. The prostate contour on the CT component was first copied to the registered PET component. Starting from the SUVmax location within the prostate contour, rectangular boxes were consecutively expanded by adding a thickness of one voxel to the box at each iteration. All voxels with SUV larger or equal to the %SUVmax threshold were added to the new GTV. A new voxel was added to the structure only

if one of its six neighbours was already in the new GTV. The box expansion was stopped once no new voxels were added to the GTV. The resulting GTV was post-processed to fill holes in the structure. GTVs were constructed for a range of %SUVmax threshold = [5%, 95%] with 5% step size, resulting in 19 GTVs per patient. Structure creation was performed by using the SimpleITK module in Python. Resulting GTVs were imported back to the TPS for metric extraction.

In the context of BgRT, dose delivery is triggered from PET emission originating from a volume called the biological tracking zone (BTZ) [11,12]. BTZ size may be varied depending on the treated site. The BTZ was modelled by generating three-dimensional shell of thickness 5 mm/10 mm/20 mm from isotropic outer margin expansion of all GTVs. Suitability to BgRT requires a strong signal-to-background ratio originating from the GTV. The normalised SUV (nSUV) was calculated to characterize this signal. nSUV was defined as the ratio of SUVmax inside the GTV to SUVmean inside the generated 3D shell expansion.

A tumour was deemed suitable for BgRT if two conditions were met. First, nSUV had to be larger or equal to an nSUV threshold (nSUVt) to ensure a sufficiently strong signal-to-background ratio. The value of this threshold is not yet established and may be varied depending on the treated site and the radiotracer used. We therefore chose to show results for values of nSUVt = 2.7/3/3.3 as trade-off between the strength of the signal-to-background ratio and the number of tumours that may satisfy this condition.

Second, the BTZ had to be free of PSMA uptake originating from any non-tumour tissue. In this context, PSMA uptake surrounding the tumour is typically located in the bladder. In order to quantify the proportion of BTZs free from non-tumour PSMA uptake, the distance between the GTV and the bladder was obtained and the distribution of PSMA uptake around the GTV was quantified. The distance between the GTV and the bladder was determined by generating successive margin expansions of the GTV. The smallest value of GTV margin expansion overlapping with the bladder contour was assessed as the distance between the GTV and the bladder. The distribution of PSMA uptake surrounding the GTV was characterized by the generation of three-dimensional shells with fixed 3 mm thickness generated at distances = [3 mm, 30 mm] with 1 mm step size. SUVmax inside all shells was determined. The presence of bladder uptake was identified by two consecutives increases of SUVmax and reported as a function of the distance from the outer layer of the first shell to the GTV.

Differences between distributions were characterized by using the Wilcoxon rank sum test. The null hypothesis that medians are similar was rejected at the 95% statistical level. Statistical correlations were calculated by using the Spearman correlation coefficient and its associated p-value.

Results

The cohort consisted of 84 patients imaged at our institution. The PET/CT scan was incomplete in one patient. Therefore, 83 primary tumours were included. In this cohort, 60 (71%) patients were diagnosed with N0M0 disease. In the remaining patients, 12 (14%) patients were diagnosed with nodal disease and distant metastasis disease (N1M1), 8 (10%) patients with nodal disease only (N1M0), and 4 (5%) patients with metastatic disease only (N0M1). This patient subset was representative of the multicentre ProPSMA cohort [40] and was similar to another prostate cancer staging study [42].

Registration of the SUV uptake on the PET component to the CT component was of the order of the PET resolution (median 3D shift = 2.9 mm; IQR = 0.9 mm – 4.8 mm). Prostate volume ranged from 19 cm^3 to 148 cm^3 (median = 52 cm^3; IQR = 39 cm^3– 63 cm^3). SUVmax inside the prostate was between 2 and 125 (median = 19; IQR = 11 – 30). The correlation between prostate volume and SUVmax inside the prostate was not statistically significant (p-value = 0.24).

Figure 1(a) shows an example of GTVs obtained from different % SUVmax thresholds. The distribution of GTV volumes for each %
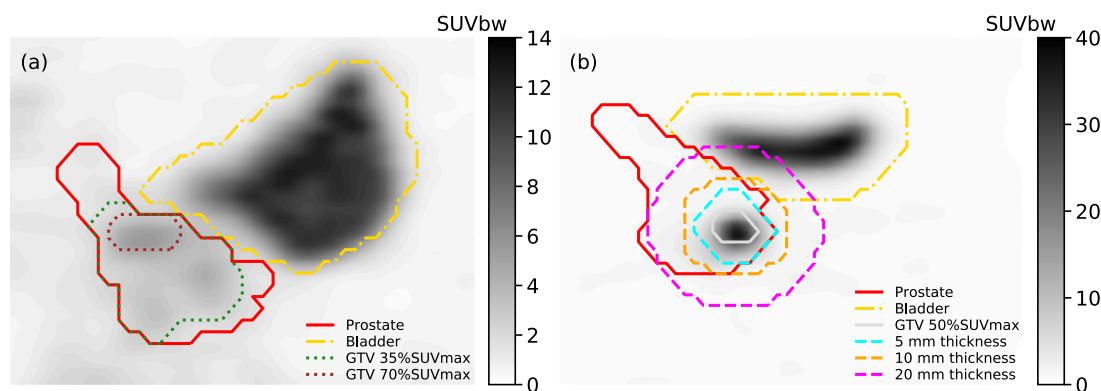
Fig. 1. (a) Example of GTV obtained from two %SUVmax thresholds. (b) Illustration of 5 mm/10 mm/20 mm shell thickness used to model BTZ.

SUVmax threshold is summarized in the Supplementary Material. The number of generated GTVs decreased for %SUVmax threshold $\geq 70\%$ as structures obtained with high threshold values involved few voxels and were not recognized as valid structures by the TPS. Resulting GTV volumes for all %SUVmax thresholds ranged from 0.002 cm^3 to 136 cm^3. All differences in GTV volume median were statistically significant for all %SUVmax thresholds (p-value = [10^{-9}, 0.046]), except between 25% SUVmax and 30%SUVmax, 30%SUVmax and 35%SUVmax, and 35% SUVmax and 40%SUVmax (all three with p-value = 0.08).

An example of the three dimensional shells involved in the nSUV calculation is shown in Fig. 1(b). The distribution of nSUV for shell of thickness of 5 mm/10 mm/20 mm is shown in the Supplementary Material for each %SUVmax threshold. For a fixed shell thickness and a given patient, and assuming the absence of an avid region in the surrounding tissue, an increase in %SUVmax threshold resulted in a smaller GTV volume and to a larger SUVmean inside the shell. This increase in SUVmean led to a decrease in nSUV since SUVmax inside the target was the same in all GTV volumes for a given patient.

A similar rationale applies as the shell thickness is increased for a fixed %SUVmax threshold volume. If the absence of an avid region in tissue surrounding the tumour is assumed, increasing the shell thickness decreased SUVmean as more low SUV values were considered in the calculation, which increased nSUV. However, high SUV values may be included in the calculation of SUVmean if they arise from avid regions adjacent to the tumour, which decreased nSUV. This situation was likely to occur for large shell thickness.

The proximity of the bladder was quantified to determine suitability to BgRT. The distribution of distances between the bladder and GTV is shown in the Supplementary Material for each %SUVmax threshold considered. However, it is the PET emission originating from the bladder that may impact BgRT delivery, therefore this may be considered as a lower bound on the distances.

The proportion of tumours suitable for BgRT (nSUV $\geq$ nSUVt and BTZ free of PET uptake) is shown in Fig. 2 and is further detailed in the Supplementary Material for three GTV margin expansions and three nSUV thresholds. On the one hand, the distance between the GTV and the bladder PET uptake increased as the %SUVmax threshold was increased, which increased the proportion of tumours suitable for BgRT. On the other hand, nSUV decreased as the %SUVmax threshold was increased since more high SUV values are included in the calculation of SUV mean, which decreased the proportion of tumours suitable for BgRT. The combination of these two processes led to an optimal value % SUVmax threshold that maximized the proportion of tumours suitable for BgRT.

By using a margin expansion of 5 mm, the proportion of tumours suitable for BgRT was maximized with the 50%SUVmax/35%SUVmax/ 35%SUVmax threshold for nSUVt of 2.7/3/3.3 (76%/72%/71% of tumours were suitable). The proportion decreased as the margin expansion

was increased to 10 mm. In this case, 69%/64%/63% of tumours were suitable by using the 70%SUVmax/55%SUVmax/55%SUVmax threshold and nSUVt of 2.7/3/3.3. The proportion of tumours suitable for BgRT was less than 35% for all nSUV considered with a margin expansion of 20 mm. This is due to the proximity of the PET uptake originating from the bladder since the bladder contour was within 15 mm for all GTVs considered.

Discussion

For prostate cancer, BgRT can potentially allow targeting of the DIL. In most centres, fiducial markers are inserted into the prostate prior the commencement of radiotherapy and subsequently used to localize the prostate prior irradiation. However, during the course of radiotherapy, the prostate can change in shape, decline in volume, and fiducial markers can migrate [43]. Such changes may be acceptable when irradiating the prostate with a margin but for DIL boost where either a much smaller margin or no margins are applied [7], a more accurate strategy, such as BgRT, may be required. BgRT relies on radionuclide emissions from tumour to direct radiotherapy and therefore is adaptable to the day-to-day variations in the size and shape of the prostate and in the DIL location. Furthermore, localization of the target via PSMA radionuclide emission would be independent of the fiducial markers and their migration. Moreover, BgRT would involve the administration of radiotracers prior to each fraction of radiotherapy. As a result, BgRT would be best suited to ultra-hypofractionated treatments rather than conventional fractionated radiotherapy. Therefore, BgRT treatment could be beneficial to a subset of patients with synchronous oligometastatic disease since future development envisions that all lesions, including boost to the DIL, can be irradiated in a single session, and consequently reducing the overall treatment time as compared with a standard SABR approach. In the ProPSMA cohort considered in this study, 24/84 (29%) patients had synchronous oligometastatic disease.

GTVs were generated from a %SUVmax threshold technique. Recent DIL volume determinations from PSMA PET scan in the literature are summarized in Table 1 [29,33,34,36]. GTVs generated with the 25% SUVmax threshold in this study best matched the median and interquartile of DIL volumes determined from histopathology (n = 47 patients) [33,34,38] whereas the 50%SUVmax threshold best matched the mean, 95% confidence interval and range of DIL volumes determined from mpMRI (n = 1205 patients) [27].

The feasibility of BgRT sequential boost to PSMA avid subvolumes in the prostate region was investigated in this study. The suitability of BgRT requires a high signal-to-background ratio, quantified in this study through the calculation of the nSUV, and a BTZ free from PSMA uptake, to spare organs at risk with PET uptake from dose delivery. With nSUVt = 3, more than 50% of all GTVs were suitable for BgRT by using a % SUVmax threshold between 20% and 50% with the margin expansion of
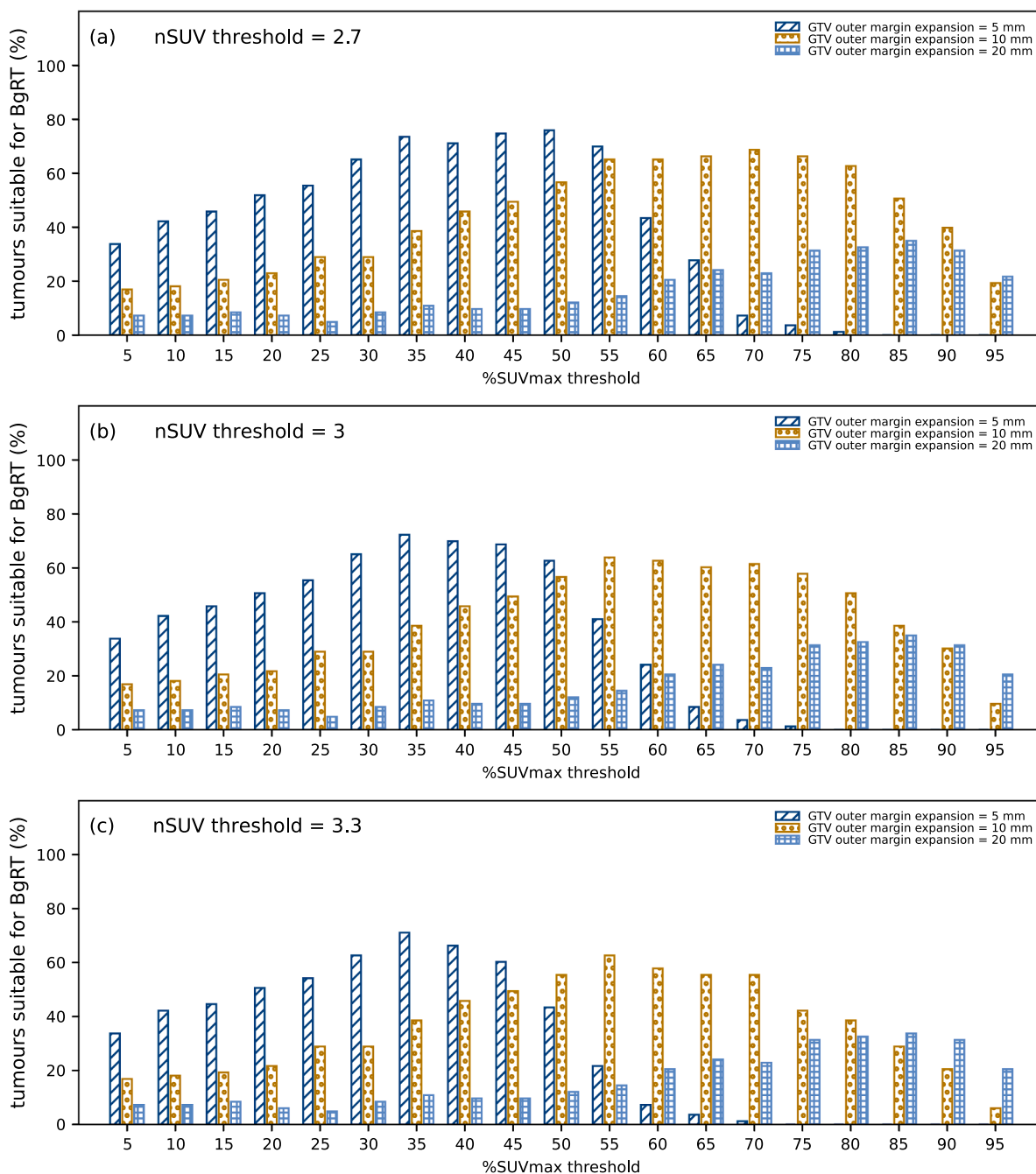
Fig. 2. Proportion of tumours suitable for BgRT (nSUV $\geq$ nSUV threshold and BTZ free of PET uptake) for each %SUVmax threshold considered by using a margin expansion of 5 mm/10 mm/20 mm. Results are shown for nSUV threshold of (a) 2.7, (b) 3, and (c) 3.3.

Table 1
Summary of median and interquartile (IQR) DIL volume (cm^3) determined from %SUVmax threshold on PSMA PET scan in recent studies.

Study	Reference	%SUVmax threshold	Median DIL volume (cm^3)	IQR DIL volume (cm^3)
Sasidharan et al.	[29]	30%−40%	4	2.5–7.6
Spohn et al.	[33]	20%	3.9	1.0–25.5
		30%	2.6	0.6–20.0
		40%	1.7	0.4–10.2
		50%	1.2	0.3–4.2
Zamboglou et al.	[34]	20%	17.5	12.5–37.2
		30%	8	3.1–19.9
		40%	3.9	1.5–10.5
		50%	1.4	0.8–3.7
Goodman et al.	[35]	23%−40%	1	0.42–1.83

5 mm and between 50% and 80% with the margin expansion of 10 mm. However, BTZs generated from the GTV margin expansion of 20 mm was found to be to large due to the proximity of bladder uptake (less than 35% of all GTVs were suitable for BgRT by using a margin expansion of 20 mm).

Therefore, it is feasible to identify suitable candidates to BgRT sequential boost to the PSMA avid subvolumes in the prostate region. These GTVs are characterized by a small volume, a strong PSMA signal-to-background, and a location far from the bladder uptake.

The major limitation of this study is the absence of histopathology samples and MRI datasets from which DIL volume could have been verified. mpMRI is the current standard in DIL determination and this imaging technique has been shown to outperform PSMA PET in the detection of extraprostatic extension and seminal vesicle invasion of prostate cancer [44]. However, when compared to histologically derived DIL, PSMA PET has been previously shown to demonstrate 75% sensitivity and 87% specificity, which was comparable to that of MRI [45]. Ideally, both mpMRI and PSMA PET would be used to identify the tumour. With this in mind, our results indicate that a range of %SUVmax threshold would also have led to a high proportion of tumours suitable for BgRT, as detailed in Table S2 of the Supplementary Material. It is worth to note that automatic delineation on PSMA PET based on deep-learning architecture may have the potential to eliminate the uncertainty related to which %SUVmax threshold best match the tumour [46,47].

Furthermore, the nSUV threshold that ensures a sufficiently strong signal-to-background ratio is not yet established and an interval of plausible values was arbitrarily selected. It was assumed that the PET signal remained constant during the course of treatment. A decrease in SUVmax and or an increase in SUVmean post-radiation would result in a lower nSUV, which may compromise the suitability of this tumour for the subsequent BgRT fractions.

Moreover, presence of PSMA bladder uptake may affect BgRT delivery. Use of PET tracer with lower renal clearance such as ^{18}F-PSMA-1007 or longer half-life, such as ^{46}CuPSMA PET tracer, or interventions such as administration of frusemide, may help reduce PET emission originating from the bladder and increase the number of DILs that are suitable for BgRT [48,49].

Finally, the ProPSMA clinical trial only included men with biopsy-proven prostate cancer and high-risk features. It has been demonstrated that SUVmax values of high-risk patients are statistically higher than those of low-risk patients [50]. Assuming similar SUV background in the two groups, it is expected that nSUV values would be lower in a cohort of low-risk patients and therefore less tumours may be suitable for BgRT.

Conclusions

BgRT delivery as a sequential boost to PSMA avid subvolume in the prostate region is feasible. More than 50% PSMA-avid subvolumes in the prostate region in the subset of ProPSMA patients treated at our institution were suitable for BgRT due to their large signal-to-background ratio and the absence of bladder PSMA uptake in the delivery volume.

Declaration of Competing Interest

The authors declare the following financial interests/personal relationships which may be considered as potential competing interests:
This research is partially funded by RefleXion Medical.

Acknowledgements

Appendix A. Supplementary data

Supplementary data to this article can be found online at https://doi.org/10.1016/j.ctro.2022.05.005.

References

[1] Einspieler I, Rauscher I, Düwel C, Krönke M, Rischpler C, Habl G, et al. Detection efficacy of hybrid 68Ga-PSMA ligand PET/CT in prostate cancer patients with biochemical recurrence after primary radiation therapy defined by phoenix criteria. J Nucl Med 2017;58:1081–7.

[2] Hruby G, Eade T, Kneebone A, Emmett L, Guo L, Ho B, et al. Delineating biochemical failure with 68Ga-PSMA-PET following definitive external beam radiation treatment for prostate cancer. Radiother Oncol 2017;122:99–102.

[3] Philippou Y, Parker RA, Volanis D, Gnanapragasam VJ. Comparative oncologic and toxicity outcomes of salvage radical prostatectomy versus nonsurgical therapies for radiorecurrent prostate cancer: a meta-regression analysis. Eur Urol Focus 2016;2:158–71.

[4] Valle LF, Lehrer EJ, Markovic D, Elashoff D, Levin-Epstein R, Karnes RJ, et al. A systematic review and meta-analysis of local salvage therapies after radiotherapy for prostate cancer (MASTER)[Formula presented]. Eur Urol 2021;80:280–92.

[5] Ahmed HU, Hindley RG, Dickinson L, Freeman A, Kirkham AP, Sahu M, et al. Focal therapy for localised unifocal and multifocal prostate cancer: a prospective development study. Available from Lancet Oncol [Internet] 2012;13:622–32. http://www.ncbi.nlm.nih.gov/pubmed/22512844.

[6] Pucar D, Hricak H, Shukla-Dave A, Kuroiwa K, Drobnjak M, Eastham J, et al. {A figure is presented}Clinically significant prostate cancer local recurrence after radiation therapy occurs at the site of primary tumor: magnetic resonance imaging and step-section pathology evidence. Int J Radiat Oncol Biol Phys 2007;69:62–9.

[7] Kerkmeijer LGW, Groen VH, Pos FJ, Haustermans K, Monninkhof EM, Smeenk RJ, et al. Focal boost to the intraprostatic tumor in external beam radiotherapy for patients with localized prostate cancer: results from the FLAME randomized phase III trial. J Clin Oncol 2021;39:787–96.

[8] Evans PM. Anatomical imaging for radiotherapy. Phys Med Biol 2008;53.

[9] Nestle U, Weber W, Hentschel M, Grosu AL. Biological imaging in radiation therapy: role of positron emission tomography. Phys Med Biol 2009;54.

[10] Verellen D, de Ridder M, Storme G. A (short) history of image-guided radiotherapy. Radiother Oncol 2008;86:4–13.

[11] Shirvani SM, Huntzinger CJ, Melcher T, Olcott PD, Voronenko Y, Bartlett-Roberto J, et al. Biology-guided radiotherapy: redefining the role of radiotherapy in metastatic cancer. Br J Radiol 2021;94:20200873.

[12] Oderinde OM, Shirvani SM, Olcott PD, Kuduvalli G, Mazin S, Larkin D. The technical design and concept of a PET/CT linac for biology-guided radiotherapy. Clinical and Translational Radiation Oncology [Internet]. RefleXion Medical; 2021;29:1–7. Available from: https://doi.org/10.1016/j.ctro.2021.04.003.

[13] Yang J, Yamamoto T, Mazin SR, Graves EE, Keall PJ. The potential of positron emission tomography for intratreatment dynamic lung tumor tracking: a phantom study. Med Phys 2014;41.

[14] Fan Q, Nanduri A, Mazin S, Zhu L. Emission guided radiation therapy for lung and prostate cancers: a feasibility study on a digital patient. Med Phys 2012;39:7140–52.

[15] Cho SY, Szabo Z. Molecular imaging of urogenital diseases. Semin Nucl Med, Elsevier 2014;44:93–109.

[16] Tosoian JJ, Gorin MA, Ross AE, Pienta KJ, Tran PT, Schaeffer EM, et al. and Treatment Considerations. 2018;14:15–25.

[17] van Leeuwen PJ, Stricker P, Hruby G, Kneebone A, Ting F, Thompson B, et al. 68Ga-PSMA has a high detection rate of prostate cancer recurrence outside the prostatic fossa in patients being considered for salvage radiation treatment. BJU Int 2016;117:732–9.

[18] Eiber M, Fendler WP, Rowe SP, Calais J, Hofman MS, Maurer T, et al. Prostate-specific membrane antigen ligands for imaging and therapy. J Nucl Med 2017;58:67S–76S.

[19] Hofman MS, Iravani A, Nzenza T, Murphy DG. Advances in urologic imaging: prostate-specific membrane antigen ligand PET imaging. Urol Clin North Am 2018;45:503–24.

[20] Hofman MS, Hicks RJ, Maurer T, Eiber M. Prostate-specific membrane antigen PET: clinical utility in prostate cancer, normal patterns, pearls, and pitfalls. Radiographics 2018;38:200–17.

[21] Perera M, Papa N, Roberts M, Williams M, Udovicich C, Vela I, et al. Gallium-68 prostate-specific membrane antigen positron emission tomography in advanced prostate cancer—updated diagnostic utility, sensitivity, specificity, and distribution of prostate-specific membrane antigen-avid lesions: a systematic review and meta-. Available from Eur Urol [Internet] 2020;77:403–17. https://linkinghub.elsevier.com/retrieve/pii/S0302283819300958.

[22] Morris MJ, Rowe SP, Gorin MA, Saperstein L, Pouliot F, Josephson D, et al. Diagnostic performance of 18 F-DCFPyL-PET/CT in men with biochemically

recurrent prostate cancer: results from the CONDOR phase III, multicenter study. Available from Clin Cancer Res [Internet] 2021;27:3674–82. http://clincancerres.aacrjournals.org/lookup/doi/10.1158/1078-0432.CCR-20-4573.

[23] Hofman MS, Murphy DG, Williams SG, Nzenza T, Herschtal A, de Abreu LR, et al. A prospective randomized multicentre study of the impact of gallium-68 prostate-specific membrane antigen (PSMA) PET/CT imaging for staging high-risk prostate cancer prior to curative-intent surgery or radiotherapy (proPSMA study): clinical trial protocol. BJU Int 2018;122:783–93.

[24] Murray JR, Tree AC, Alexander EJ, Sohaib A, Hazell S, Thomas K, et al. Standard and hypofractionated dose escalation to intraprostatic tumor nodules in localized prostate cancer: efficacy and toxicity in the DELINEATE trial. Int J Radiat Oncol Biol Phys 2020;106:715–24.

[25] Feutren T, Herrera FG. Prostate irradiation with focal dose escalation to the intraprostatic dominant nodule: a systematic review. Prostate Int 2018;6:75–87.

[26] Bauman G, Haider M, van der Heide UA, Ménard C. Boosting imaging defined dominant prostatic tumors: a systematic review. Radiother Oncol 2013;107:274–81.

[27] von Eyben FE, Kiljunen T, Kangasmaki A, Kairemo K, von Eyben R, Joensuu T. Radiotherapy Boost for the Dominant Intraprostatic Cancer Lesion - A Systematic Review and Meta-Analysis. Clinical Genitourinary Cancer [Internet]. Elsevier Inc.; 2016;14:189–97. Available from: https://doi.org/10.1016/j.clgc.2015.12.005.

[28] van der Leest M, Israël B, Cornel EB, Zámecnik P, Schoots IG, van der Lelij H, et al. High diagnostic performance of short magnetic resonance imaging protocols for prostate cancer detection in biopsy-naïve men: the next step in magnetic resonance imaging accessibility. Eur Urol 2019;76:574–81.

[29] Sasidharan A, Murthy V, Natarajan A, Agarwal A, Ranagrajan V, Gudi S, et al. Pilot study comparing dominant intraprostatic lesion volume using Ga-68 prostate-specific membrane antigen PET-computed tomography and multiparametric MRI. Nucl Med Commun 2020:1291–8.

[30] Zamboglou C, Klein CM, Thomann B, Fassbender TF, Rischke HC, Kirste S, et al. The dose distribution in dominant intraprostatic tumour lesions defined by multiparametric MRI and PSMA PET/CT correlates with the outcome in patients treated with primary radiation therapy for prostate cancer. Radiat Oncol 2018;13.

[31] Scobioala S, Kittel C, Wolters H, Huss S, Elsayad K, Seifert R, et al. Diagnostic efficiency of hybrid imaging using PSMA ligands, PET/CT, PET/MRI and MRI in identifying malignant prostate lesions. Ann Nucl Med 2021;35:628–38.

[32] Hearn N, Blazak J, Vivian P, Vignarajah D, Cahill K, Atwell D, et al. Prostate cancer GTV delineation with biparametric MRI and 68Ga-PSMA-PET: comparison of expert contours and semi-automated methods. Br J Radiol 2021;94:20201174.

[33] Spohn SKB, Kramer M, Kiefer S, Bronsert P, Sigle A, Schultze-Seemann W, et al. Comparison of manual and semi-automatic [18F]PSMA-1007 PET based contouring techniques for intraprostatic tumor delineation in patients with primary cancer and validation with histopathology as standard of reference. Front Oncol 2020;10.

[34] Zamboglou C, Fassbender TF, Steffan L, Schiller F, Fechter T, Carles M, et al. Validation of different PSMA-PET/CT-based contouring techniques for intraprostatic tumor definition using histopathology as standard of reference. Radiotherapy and Oncology [Internet]. Elsevier B.V.; 2019;141:208–13. Available from: https://doi.org/10.1016/j.radonc.2019.07.002.

[35] Draulans C, de Roover R, van der Heide UA, Kerkmeijer L, Smeenk RJ, Pos F, et al. Optimal 68Ga-PSMA and 18F-PSMA PET window levelling for gross tumour volume delineation in primary prostate cancer. Available from Eur J Nucl Med Mol Imaging [Internet] 2021;48:1211–8. https://link.springer.com/10.1007/s00259-020-05059-4.

[36] Goodman CD, Fakir H, Pautler S, Chin J, Bauman GS. Dosimetric evaluation of PSMA PET-delineated dominant intraprostatic lesion simultaneous infield boosts. Adv Radiat Oncol [Internet]. The Author(s); 2020;5:212–20. Available from: https://doi.org/10.1016/j.adro.2019.09.004.

[37] Eiber M, Weirich G, Holzapfel K, Souvatzoglou M, Haller B, Rauscher I, et al. Simultaneous 68Ga-PSMA HBED-CC PET/MRI improves the localization of primary prostate cancer. Eur Urol 2016;70:829–36.

[38] Bettermann AS, Zamboglou C, Kiefer S, Jilg CA, Spohn S, Kranz-Rudolph J, et al. [68Ga-]PSMA-11 PET/CT and multiparametric MRI for gross tumor volume delineation in a slice by slice analysis with whole mount histopathology as a reference standard – Implications for focal radiotherapy planning in primary prostate cancer. Radiother Oncol [Internet]. Elsevier B.V.; 2019;141:214–9. Available from: https://doi.org/10.1016/j.radonc.2019.07.005.

[39] Tulsyan S, Das CJ, Tripathi M, Seth A, Kumar R, Bal C. Comparison of 68 Ga-PSMA PET/CT and multiparametric MRI for staging of high-risk prostate cancer 68 Ga-PSMA PET and MRI in prostate cancer. Nucl Med Commun 2017;38:1094–102.

[40] Hofman MS, Lawrentschuk N, Francis RJ, Tang C, Vela I, Thomas P, et al. Prostate-specific membrane antigen PET-CT in patients with high-risk prostate cancer before curative-intent surgery or radiotherapy (proPSMA): a prospective, randomised, multicentre study. Available from Lancet [Internet] 2020;395:1208–16. https://linkinghub.elsevier.com/retrieve/pii/S0140673620303147.

[41] Bailey DL, Hofman MS, Forwood NJ, O'Keefe GJ, Scott AM, van Wyngaardt WM, et al. Accuracy of dose calibrators for 68Ga PET imaging: Unexpected findings in a multicenter clinical pretrial assessment. J Nucl Med 2018;59:636–8.

[42] Maurer T, Gschwend JE, Rauscher I, Souvatzoglou M, Haller B, Weirich G, et al. Diagnostic efficacy of 68Gallium-PSMA positron emission tomography compared to conventional imaging for lymph node staging of 130 consecutive patients with intermediate to high risk prostate cancer. J Urol 2016;195:1436–43.

[43] Nichol AM, Brock KK, Lockwood GA, Moseley DJ, Rosewall T, Warde PR, et al. A magnetic resonance imaging study of prostate deformation relative to implanted gold fiducial markers. Int J Radiat Oncol Biol Phys 2007;67:48–56.

[44] Sonni I, Felker ER, Lenis AT, Sisk AE, Bahri S, Allen-Auerbach MS, et al. Head-to-head comparison of 68 Ga-PSMA-11 PET/CT and mpMRI with histopathology gold-standard in the detection, intra-prostatic localization and local extension of primary prostate cancer: results from a prospective single-center imaging trial. J Nucl Med 2021;jnumed.121.262398.

[45] Zamboglou C, Drendel V, Jilg CA, Rischke HC, Beck TI, Schultze-Seemann W, et al. Comparison of 68Ga-HBED-CC PSMA-PET/CT and multiparametric MRI for gross tumour volume detection in patients with primary prostate cancer based on slice by slice comparison with histopathology. Theranostics 2017;7:228–37.

[46] Matkovic LA, Wang T, Lei Y, Akin-Akintayo OO, Abiodun Ojo OA, Akintayo AA, et al. Prostate and dominant intraprostatic lesion segmentation on PET/CT using cascaded regional-net. Phys Med Biol 2021;66.

[47] Kostyszyn D, Fechter T, Bartl N, Grosu AL, Gratzke C, Sigle A, et al. Intraprostatic tumor segmentation on PSMA PET images in patients with primary prostate cancer with a convolutional neural network. J Nucl Med 2021;62:823–8.

[48] Kesch C, Kratochwil C, Mier W, Kopka K, Giesel FL. 68Ga or 18F for prostate cancer imaging? J Nucl Med 2017;58:687–8.

[49] Rahbar K, Weckesser M, Ahmadzadehfar H, Schäfers M, Stegger L, Bögemann M. Advantage of 18F-PSMA-1007 over 68Ga-PSMA-11 PET imaging for differentiation of local recurrence vs. urinary tracer excretion. Eur J Nucl Med Mol Imaging 2018;45:1076–7.

[50] Demirci E, Kabasakal L, Şahin OE, Akgün E, Gültekin MH, Doğanca T, et al. Can SUVmax values of Ga-68-PSMA PET/CT scan predict the clinically significant prostate cancer? Nucl Med Commun 2019;40:86–91.